HHS Public Access

Author manuscript

Phys Med. Author manuscript; available in PMC 2016 July 19.

Published in final edited form as:

Phys Med. 2016 April ; 32(4): 631–635. doi:10.1016/j.ejmp.2016.03.014.

Potential of using cerium oxide nanoparticles for protecting healthy tissue during accelerated partial breast irradiation (APBI)

Zi Ouyang[a,*,1], **Madan Kumar Mainali**[b,1], **Neeharika Sinha**[c], **Guinevere Strack**[a], **Yucel Altundal**[a], **Yao Hao**[a], **Thomas Andrew Winningham**[d], **Erno Sajo**[a], **Jonathan Celli**[b], and **Wilfred Ngwa**[a,e]

[a] University of Massachusetts Lowell, Lowell, MA, USA

[b] University of Massachusetts Boston, Boston, MA, USA

[c] Wentworth Institute of Technology, Boston, MA, USA

[d] Space Coast Cancer Center, Titusville, FL, USA

[e] Brigham and Women's Hospital, Dana-Farber Cancer Institute and Harvard Medical School, Boston, MA, USA

Abstract

The purpose of this study is to investigate the feasibility of using cerium oxide nanoparticles (CONPs) as radical scavengers during accelerated partial breast irradiation (APBI) to protect normal tissue. We hypothesize that CONPs can be slowly released from the routinely used APBI balloon applicators—via a degradable coating—and protect the normal tissue on the border of the lumpectomy cavity over the duration of APBI. To assess the feasibility of this approach, we analytically calculated the initial concentration of CONPs required to protect normal breast tissue from reactive oxygen species (ROS) and the time required for the particles to diffuse to various distances from the lumpectomy wall. Given that cerium has a high atomic number, we took into account the possible inadvertent dose enhancement that could occur due to the photoelectric interactions with radiotherapy photons. To protect against a typical MammoSite treatment fraction of 3.4 Gy, 5 ng-g^{-1} of CONPs is required to scavenge hydroxyl radicals and hydrogen peroxide. Using 2 nm sized NPs, with an initial concentration of 1 mg-g^{-1}, we found that 2–10 days of diffusion is required to obtain desired concentrations of CONPs in regions 1–2 cm away from the lumpectomy wall. The resultant dose enhancement factor (DEF) is less than 1.01 under such conditions. Our results predict that CONPs can be employed for radioprotection during APBI using a new design in which balloon applicators are coated with the NPs for sustained/controlled in-situ release from within the lumpectomy cavity.

* Corresponding author at: Department of Physics and Applied Physics, University of Massachusetts Lowell, 1 University Ave, Lowell, MA 01854, USA. Zi_Ouyang@student.uml.edu (Z. Ouyang).

[1] Co-first authors.

Keywords

APBI; Cerium oxide; Radiolysis; Radioprotectant

Introduction

Breast cancer is the second most common type of non-skin cancer (after lung cancer) and the fifth most common cause of cancer death. Recent surveillance epidemiology and end results indicate that 60.8% of diagnosed breast cancers were in stage I (localized stage). The five-year survival rates for stage I and overall breast cancer in 2004–2010 were 98.5% and 89.2%, respectively [1,2]. These statistics suggest a need for improvement in the clinical management of early-stage breast cancer. One promising clinical practice, accelerated partial breast irradiation (APBI), is a cancer management technique that involves the surgical removal of the tumor, followed by the irradiation of the lumpectomy bed at a depth of 1–2 cm. The radiation treatment period is less than five weeks—with daily fraction doses greater than two Gy—and employs low-energy radiation sources, including isotopic sources and 50 kVp electronic brachytherapy *x*-radiation [2].

During cancer treatment, radiotherapy photons induce the radiolysis of tissue that generates reactive oxygen species (ROS) that can damage DNA and lead to cell death [3,4]. Although the radiolysis of water results in the generation of several ROS—including hydroxyl radicals (OH·) and hydrogen peroxide (H_2O_2)—hydroxyl radicals inflict the majority of the unrepairable DNA damage [3]. Unfortunately, radiotherapy not only inflicts damage to cancer cells, it also inflicts damage to surrounding normal tissue and causes several side effects, including skin irritation, loss of appetite, fatigue, and nausea [3]. Traditionally, amifostine, vitamin E, ascorbate, carotenes, melatonin, and lipoic acid derivatives have been used or investigated as normal cell protectants. However, these antioxidants and radical scavengers have had limited success due to their short pharmacokinetic half-life, lack of penetration to the radical production site, high cost, and side effects such as nausea, vomiting, and hypotension [5,6]. Therefore, research—and identification of novel compounds that can address the drawbacks of clinically available radiation protectants and can improve the efficacy and therapeutic index in cancer treatment—is required.

Nanoparticle (NP) aided radiotherapy is a rapidly growing field with a variety of promising applications ranging from targeted dose enhancement to selective radioprotection [7]. In particular, *in vitro* studies have shown that cerium oxide nanoparticles (CONPs) are viable candidates for the selective protection of normal cells from the harmful effects of radiation during radiotherapy [8]. Cell protection is a result of the catalytic removal of ROS and prevents the subsequent ROS-induced apoptosis in normal cells [9]. CONPs remove ROS from solution using intrinsic biomimetic catalytic properties, e.g., superoxide and catalase mimetic activities. Moreover, CONPs have been shown to catalytically remove OH· from solution [10]. This is of particular importance, considering that OH· possess a relatively high radiolytic yield and inflict substantial damage to DNA [3].

Although the exact catalytic mechanism behind the removal of each ROS from solution remains unclear, the catalytic properties of CONPs are due to the rapid, reversible

transformation of the oxidation state between Ce^{3+} and Ce^{4+}, Fig. 1. This occurs due to the 30% lower oxygen vacancy formation energy on the surface of ceria compared to the bulk, which suggests that oxygen exchange between adsorbed species and the ceria surface can occur. When one oxygen vacancy is created, two adjacent Ce^{4+} atoms are reduced to Ce^{3+} [11]. Therefore, the valence state and intrinsic oxygen defects, along with the partial pressure of oxygen in the surrounding media, allow CONPs to serve as auto-regenerative redox status modulators [12]. Other factors that dictate the extent of the reversible cycling between the Ce^{3+} and Ce^{4+} redox state of nanostructured ceria are the enhanced surface area to volume ratio, quantum confinement, and lattice parameters [13].

However, since cerium is a high-Z material ($Z = 58$), it also has a potential to enhance the radiation dose in the tissue via photoelectric interactions during APBI. A previous study [14] suggested that because of this effect, CONPs may not be used for radioprotection, especially when using kV-energy radiotherapy modalities, such as the Xoft Axxent™ electronic brachytherapy [2]. This is because, at low incident photon energies, the photoelectric cross section is large and there is a higher probability of dose enhancement. Therefore, herein, we investigate (i) the minimum concentration of CONPs needed to remove the ROS generated by the radiolysis of the water, (ii) the time required for a protective concentration CONPs to diffuse into the breast tissue, and (iii) the inadvertent dose enhancement potential of CONPs during APBI using kV-energy systems.

Methods

CONP-mediated ROS scavenging

To calculate the concentration of CONPs needed to remove the ROS produced by the radiolysis of water, we considered the two main ROS with known radiolytic yields—OH· and H_2O_2—which were taken as 0.26 μmol J^{-1} and 0.073 μmol J^{-1}, respectively [4]. The removal of ROS involves two molecules of OH· or H_2O_2 and one molecule of reduced cerium oxide in one redox cycle; the regeneration of the Ce^{3+} state was based on previous experimental work and assumed to occur 20 times for each CeO_2 molecule [15,16]. Using this information, the concentrations of CONPs required to scavenge various concentrations of OH· and H_2O_2 are estimated.

CONP diffusion

Herein, we consider a clinically feasible CONP-delivery method. The CONPs are assumed to be incorporated into a micrometre-thick polymer film on the surface of routinely used APBI balloon applicators for sustained *in-situ* release, Fig. 2 [17]. An advantage of this approach is that the release of the CONPs can be customized or controlled for sustained delivery over the duration of APBI at no additional inconvenience to the patients. In this simplified model, NPs have a steady-state isotropic initial release over time.

In modeling the diffusion of CONPs, an experimentally determined diffusion coefficient, 2.2×10^{-8} cm^2 s^{-1}, for 10 nm NPs is used to calculate the diffusion coefficients for nanoparticles of other sizes using the Stokes–Einstein diffusion formula [18]:

$$D=\frac{K_B T}{6\pi\eta r} \quad (1)$$

Here, D is the diffusion coefficient, K_B is the Boltzmann constant, T is the absolute temperature, η is the viscosity of medium, and r is the radius of spherical NPs. The diffusion coefficient is independent of the mass and solely dependent on the size of the NPs and the viscosity and temperature of the medium [19]. Although the diffusion of the CONPs in the cellular environment may be more complex, a simple model with assumed uniform diffusion is employed here as a first step. Fick's law of diffusion is used to determine the initial concentration of CONPs needed to achieve a minimum concentration for radioprotection at different distances from the lumpectomy cavity during APBI. The concentration of NPs as a function of distance, x, and time, t, for different sizes of NP is given by the solution of Fick's second law of diffusion [20]:

$$C(x,t)=C_s\left[1-erf\left(\frac{x}{2\sqrt{Dt}}\right)\right] \quad (2)$$

where C_s is the initial concentration at the wall of the lumpectomy cavity and is defined as the concentration of the CONPs present in the balloon coating; both the polymer and breast tissue are considered as water-equivalent. Here, the concentration of NPs originally present in breast tissue is assumed to be zero.

DEF

DEF is a measure of how much radiation dose enhancement results from the presence of a given drug. It is defined as

$$\mathrm{DEF}=\frac{\mathrm{Dose\ \ with\ \ drug}}{\mathrm{Dose\ \ without\ \ drug}}(\mathrm{same\ \ radiation}) \quad (3)$$

The tissue voxel model is used to calculate dose enhancement, Fig. 3 [21,22]. The empirical relation between the electron energy loss with distance traveled dE/dR (keV/μm) and the residual range R (μm) ($R = R_{tot} - r_e$) is based on Cole's formula, where R_{tot} is the total range of the electron for a kinetic energy E and r_e is the distance from the electron emission site [23]:

$$\frac{dE}{dR}=3.316(R+0.007)^{-0.435}-0.0055\quad R^{0.33}. \quad (4)$$

The energy deposited by an electron within the tissue voxel is calculated by integrating the rate of energy loss inside the interaction sphere, which is given by:

$$E_{\text{voxel}} = \int_{R_n}^{R_n+d} \frac{dE}{dr_e} dr_e. \quad (5)$$

E_{voxel} is the kinetic energy deposited in the voxel, R_n is the position of the NP, and d is the distance the electron travels within the tissue voxel ($d = R_{tot}$ if the electron stops within the tissue voxel). The assumption of uniformly distributed NPs over a voxel and immediate neighboring voxels permits the calculations to be independent of the specific location of NPs. DEF is then calculated as:

$$\text{DEF} = 1 + \frac{\text{increased dose due to NPs}}{\text{dose without NPs}} \quad (6)$$

In this study, DEF is calculated using electronic kVp sources as well as I-125 and Pd-103 isotopic sources, accounting for their respective energy spectra. The photoelectric cross sections along with the fluorescent X-ray and Auger emission probabilities of cerium are used to calculate the energy deposition in tissue [24]. The algorithm described above is then used to calculate the DEFs.

Results

Radical scavenging

Fig. 4 depicts the concentration of H_2O_2 and OH· resulting from applied radiation doses ranging from 0 to 6 Gy. According to NSABP PROTOCOL B-39, a MammoSite treatment has 3.4 Gy per fraction prescribed dose. Fig. 5 shows concentrations of cerium oxide required to provide radioprotection with a clinically relevant range of radiation dose. Therefore, a concentration of 5 ng-g^{-1} is needed to protect the target region defined as 1–2 cm from the lumpectomy wall.

CONP diffusion

In order to minimize the dose enhancement effect that is caused by the CONP's high-Z property, the initial CONP concentration is given as 1 mg-g^{-1}. The diffusion time was based on clinical schedules, i.e., 7 days. Fig. 6 shows CONP radial distributions beyond the lumpectomy cavity after 7 days for CONPs of various sizes. 10 nm NPs are not able to provide desired protection beyond 1 cm from the surface of the balloon. Since smaller NPs diffuse faster, 2 nm NPs were selected for demonstrative purposes. Fig. 7 shows that the entire target region (1–2 cm from the lumpectomy edge) can be protected within 2–10 days of diffusion.

DEF

Fig. 8 [25] depicts the dependence of DEF on X-ray energies ranging from 50 to 140 kVp with a NP concentration of 0.645 mg/g. The differences are due to the K and L edges of cerium, which are at 40 and 6 keV, respectively. In addition, DEFs for brachytherapy sources I-125 and Pd-103 were calculated using the same concentration of CONPs and were found

to be 1.0143 and 1.0141, respectively. Overall, DEF decreases as radiation energy increases because of the decreased photoelectric cross-section. A widely used APBI radiation source, Ir-192, has a negligible DEF because of its relatively high energy. Based on the previous assumptions, one can easily see the linear relation between DEF and NP concentration, which is shown in Fig. 9. The 50 kVp source and 1 mg-g^{-1} CONP concentration used in diffusion calculations resulted in a DEF of 1.0095.

Discussion

Along with many previously published studies, this work demonstrates the rationale of employing CONPs in radiation therapies and presents the possibility of applying such particles to APBI treatments. A few days are typically required after breast conserving surgery before the start of APBI. A study of 40 patients undergoing APBI using the MammoSite system revealed that the mean time required to start APBI after device placement is 6.1 days (range; 3–12 days) [26]. As shown by our results, this waiting time is sufficient for CONPs to diffuse from the balloon coating and into the surrounding tissue. In addition, the CONPs are continuously released and the protected region expands correspondingly during the typical 5–7 day APBI treatment duration. The resultant concentration gradient implies that radioprotection furthest from the lumpectomy cavity is the lowest, however, our result show that the entire treated region should have sufficient radioprotection.

Given that the highest CONP concentration is at the region near the polymer film (or the edge of the lumpectomy wall), DEF is a potential cause of concern. However, the highest calculated DEFs are less than 1.01 in any region at any time. Therefore, DEF is not a concern and should not prevent the use of CONPs for radioprotection. Furthermore, Colon et al. reported *in vitro* experiments and showed more than 10% increase in normal human colon cell viability after radiation when added with less than 20 ng-g^{-1} of CONPs [27]. This result suggests that the protection effect is much more dominant than any potential dose enhancement effect, consistent with our findings/expectations.

This research provides a foundation for more detailed investigations, e.g., a three-dimensional case in which the diffusion may not be isotropic. It is assumed that the initial CONP concentration is in steady state, i.e. the number of NPs released from the lumpectomy cavity per unit time is constant. Future work should take into consideration several non-trivial factors including, the viscosity of the suspension, particle interactions, effects of the protein corona when applied *in vivo*, and nature of the tumor—all of which can contribute to nonisotropic diffusion [20,28].

Calculating DEF using Monte Carlo simulation would give us a more accurate and precise result. However, since we are proposing to use CONPs as radioprotectants, only a net dose enhancement result on a macroscopic level is of interest. The radiation transport details are therefore ignored in our study. In the tissue voxel model, CONPs are assumed to be outside the cells. The damage caused by dose enhancement is more severe if the NPs are inside the cells or even inside the nucleus. In such cases, the DNA is closer to the NPs and is more likely to be damaged due to enhanced radiation doses. Previous experiments showed that cell

damage was dependent on the localization of CONPs along with the NP surface coating and cell line type [29]. Therefore, the next step in our work will be to address the location of the CONPs inside the cell and assess the probability of cell survival.

The complexity of the surrounding physiology and how the CONP interacts with it is not a trivial consideration, therefore catalytic selectivity should be considered along with NP size and location. The biomimetic catalysis exhibited by CONPs has been shown to be dependent on pH; previous work has demonstrated that CONP protection decreases in an acidic environment [30]. The pH dependence can be harnessed for selective protection, given that normal cells have a neutral intercellular pH and cancer cells usually have an acidic intercellular environment. This environmentally-driven catalytic selectivity suggests that CONPs may simultaneously protect normal cells and damage cancer cells. Furthermore, intracellular localization plays an important role in the cytotoxicity of CONPs; for example, experiments showed that negatively charged CONPs exhibited cytotoxicity after entering lung cancer cells (A549) and localizing in the lysosomes [29]. Although some studies have shown that CONPs are promising candidates for selective protection, additional research is required to fully understand, harness, and tailor the effect. Such work could include the use of nanoparticles with targeting moieties to enhance selectivity.

Along with our previous work where we emphasized the dose enhancement effect by gold nanoparticles (GNPs) [17], synergistic use of both GNPs and CONPs is conceivable, where one could selectively target cancer cells for dose enhancement with GNPs and normal cells with CONPs for radioprotection. Conceivable approaches could include differential diffusion using different NP sizes, or the use of selective targeting agents, amongst other strategies. Experimental results building on the results in this work and that of others are envisioned as the promising field of nanoparticle-aided radiotherapy continues to grow.

Conclusion

Our results indicate that CONPs can be employed for radioprotection during APBI, using a CONP-embedded balloon coating for sustained/controlled *in-situ* release from within the lumpectomy cavity. We also demonstrated that the CONP concentrations needed for radioprotection will not significantly enhance the RT dose in spite of the high-Z cerium oxide component. The presence of CONPs in normal breast tissue has the potential to reduce radiation side effects by eliminating ROS without causing additional damage. The release method discussed in this work is feasible, considering the lack of potential toxicity, treatment time, and patient conveniences. These findings provide impetus for further work, including experimental research towards the development of a new radiotherapy biomaterials designed for the benefit of breast cancer patients eligible for APBI.

References

1. Howlader N, Noone A, Krapcho M, Garshell J, Miller D, Altekruse S. Cancer statistics review (CSR) 1975–2012. National Cancer Institute. 2015
2. Njeh, CF.; Saunders, MW.; Langton, CM. Radiat Oncol. London, England: 2010. Accelerated partial breast irradiation (APBI): a review of available techniques; p. 5-90.

3. Hall, EJ.; Giaccia, AJ. Radiobiology for the radiologist. Wolters Kluwer Health/Lippincott Williams & Wilkins; Philadelphia: 2012.
4. Le Caër S. Water radiolysis: influence of oxide surfaces on H_2 production under ionizing radiation. Water. 2011; 3:235.
5. Beckman KB, Ames BN. The free radical theory of aging matures. Physiol Rev. 1998; 78:547–81. [PubMed: 9562038]
6. Marchioli R, Schweiger C, Levantesi G, Tavazzi L, Valagussa F. Antioxidant vitamins and prevention of cardiovascular disease: epidemiological and clinical trial data. Lipids. 2001; 36(Suppl):S53–63. [PubMed: 11837994]
7. Ngwa, W.; Kumar, R.; Sridhar, S.; Korideck, H.; Zygmanski, P.; Cormack, RA. Nanomedicine. Vol. 9. London, England: 2014. Targeted radiotherapy with gold nanoparticles: current status and future perspectives; p. 1063-82.
8. Wason MS, Colon J, Das S, Seal S, Turkson J, Zhao J, et al. Sensitization of pancreatic cancer cells to radiation by cerium oxide nanoparticle-induced ROS production. Nanomed Nanotechnol Biol Med. 2013; 9:558–69.
9. Celardo I, De Nicola M, Mandoli C, Pedersen JZ, Traversa E, Ghibelli L. Ce(3)+ ions determine redox-dependent anti-apoptotic effect of cerium oxide nanoparticles. ACS Nano. 2011; 5:4537–49. [PubMed: 21612305]
10. Xue Y, Luan Q, Yang D, Yao X, Zhou K. Direct evidence for hydroxyl radical scavenging activity of cerium oxide nanoparticles. J Phys Chem C. 2011; 115:4433–8.
11. Mullins DR. The surface chemistry of cerium oxide. Surf Sci Rep. 2015; 70:42–85.
12. Tarnuzzer RW, Colon J, Patil S, Seal S. Vacancy engineered ceria nanostructures for protection from radiation-induced cellular damage. Nano Lett. 2005; 5:2573–7. [PubMed: 16351218]
13. Deshpande S, Patil S, Kuchibhatla SV, Seal S. Size dependency variation in lattice parameter and valency states in nanocrystalline cerium oxide. Appl Phys Lett. 2005; 87:133113.
14. Briggs A, Corde S, Oktaria S, Brown R, Rosenfeld A, Lerch M, et al. Cerium oxide nanoparticles: influence of the high-Z component revealed on radioresistant 9L cell survival under X-ray irradiation. Nanomedicine. 2013; 9:1098–105. [PubMed: 23473745]
15. Lee SS, Song W, Cho M, Puppala HL, Nguyen P, Zhu H, et al. Antioxidant properties of cerium oxide nanocrystals as a function of nanocrystal diameter and surface coating. ACS Nano. 2013; 7:9693–703. [PubMed: 24079896]
16. Xu C, Qu X. Cerium oxide nanoparticle: a remarkably versatile rare earth nanomaterial for biological applications. NPG Asia Mater. 2014; 6:e90.
17. Cifter G, Chin J, Cifter F, Altundal Y, Sinha N, Sajo E, et al. Targeted radiotherapy enhancement during electronic brachytherapy of accelerated partial breast irradiation (APBI) using controlled release of gold nanoparticles. Physica Med. 2015; 31:1070–4.
18. Wong C, Stylianopoulos T, Cui J, Martin J, Chauhan VP, Jiang W, et al. Multistage nanoparticle delivery system for deep penetration into tumor tissue. Proc Nat Acad Sci USA. 2011; 108:2426–31. [PubMed: 21245339]
19. Einstein, A.; Fürth, R. Investigations on the theory of Brownian movement. Dover Publications; New York, N.Y.: 1956.
20. Sinha N, Cifter G, Sajo E, Kumar R, Sridhar S, Nguyen PL, et al. Brachytherapy application with in situ dose painting administered by gold nanoparticle eluters. Int J Radiat Oncol Biol Phys. 2015; 91:385–92. [PubMed: 25482302]
21. Altundal Y, Cifter G, Detappe A, Sajo E, Tsiamas P, Zygmanski P, et al. New potential for enhancing concomitant chemoradiotherapy with FDA approved concentrations of cisplatin via the photoelectric effect. Physica Med. 2015; 31:25–30.
22. Hao Y, Altundal Y, Moreau M, Sajo E, Kumar R, Ngwa W. Potential for enhancing external beam radiotherapy for lung cancer using high-Z nanoparticles administered via inhalation. Phys Med Biol. 2015; 60:7035. [PubMed: 26309064]
23. Cole A. Absorption of 20-eV to 50,000-eV electron beams in air and plastic. Radiat Res. 1969; 38:7–33. [PubMed: 5777999]

24. Perkins, S.; Cullen, D. CA. Lawrence Livermore National Lab; United States: 1994. ENDL type formats for the LLNL evaluated atomic data library, EADL, for the evaluated electron data library, EEDL, and for the evaluated photon data library, EPDL.

25. Siemens. Simulation of X-ray spectra

26. DiFronzo LA, Tsai PI, Hwang JM, Lee JJ, Ryoo MC, Rahimian J, et al. Breast conserving surgery and accelerated partial breast irradiation using the MammoSite system: initial clinical experience. Arch Surg. 2005; 140:787–94. [PubMed: 16103290]

27. Colon J, Hsieh N, Ferguson A, Kupelian P, Seal S, Jenkins DW, et al. Cerium oxide nanoparticles protect gastrointestinal epithelium from radiation-induced damage by reduction of reactive oxygen species and upregulation of superoxide dismutase 2. Nanomedicine. 2010; 6:698–705. [PubMed: 20172051]

28. Jain RK, Stylianopoulos T. Delivering nanomedicine to solid tumors. Nat Rev Clin Oncol. 2010; 7:653–64. [PubMed: 20838415]

29. Asati A, Santra S, Kaittanis C, Perez JM. Surface-charge-dependent cell localization and cytotoxicity of cerium oxide nanoparticles. ACS Nano. 2010; 4:5321–31. [PubMed: 20690607]

30. Perez JM, Asati A, Nath S, Kaittanis C. Synthesis of biocompatible dextran-coated nanoceria with pH-dependent antioxidant properties. Small. 2008; 4:552–6. [PubMed: 18433077]

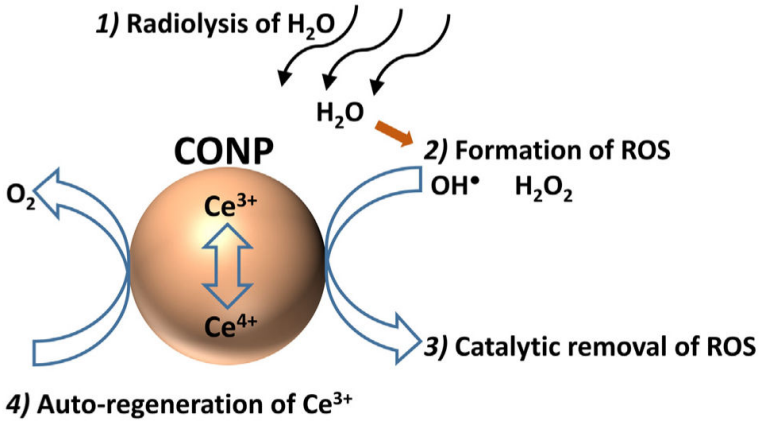

Figure 1.

Schematic of (1) water is exposed to 3.4 Gy of radiation, (2) the radiolysis of water produces ROS, namely $OH^{\cdot}$ and H_2O_2, (3) the removal of ROS from solution results in the oxidation of CONPs from Ce^{3+} to the Ce^{4+} state, (4) the auto-regeneration of the Ce^{3+} state. Please note: the chemical reactions depicted in this scheme are for conceptual purposes only; reaction mechanisms, intermediates, and products are not considered.

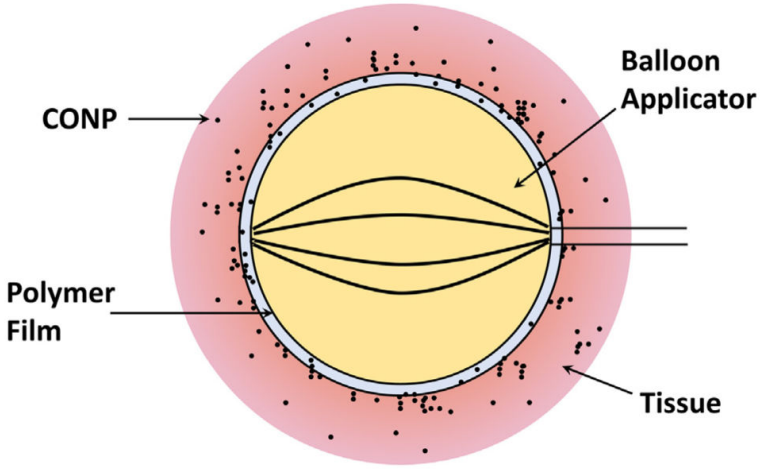

Figure 2.

Schematic diagram of APBI using a balloon applicator coated with degradable polymer loaded with CONPs. Upon implantation of the balloon applicator, the CONPs are released into the surrounding tissue to provide protection from reactive oxygen species (ROS).

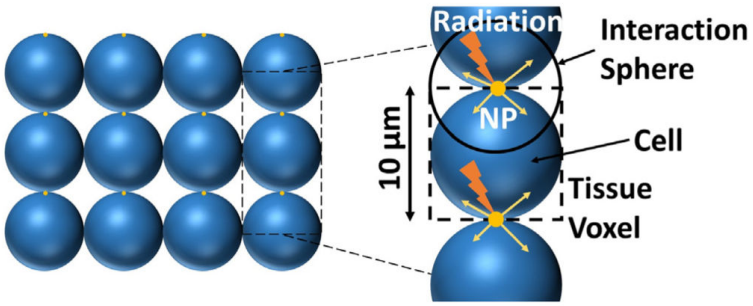

Figure 3.

Tissue voxel model used for DEF calculation. The nanoparticles are assumed to be homogeneously distributed throughout the cells ($V = 1000\ \mu m^3$).

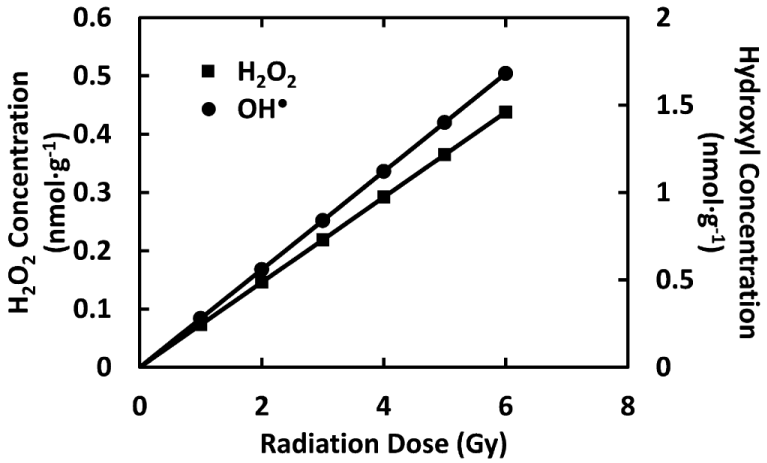

Figure 4.

H_2O_2 (left axis) and OH· (right axis) production linearly increases with respect to radiation dose.

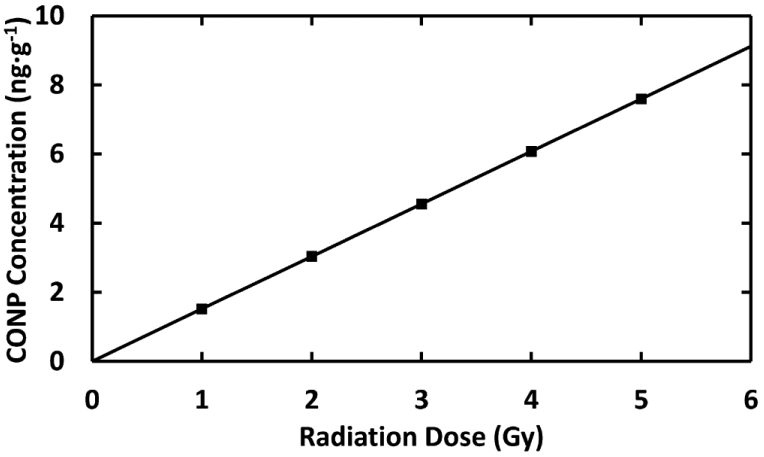

Figure 5.

The concentration of CONPs needed to eliminate most ROS in the presence of a clinically relevant a radiation dose ranging from 0 to 6 Gy.

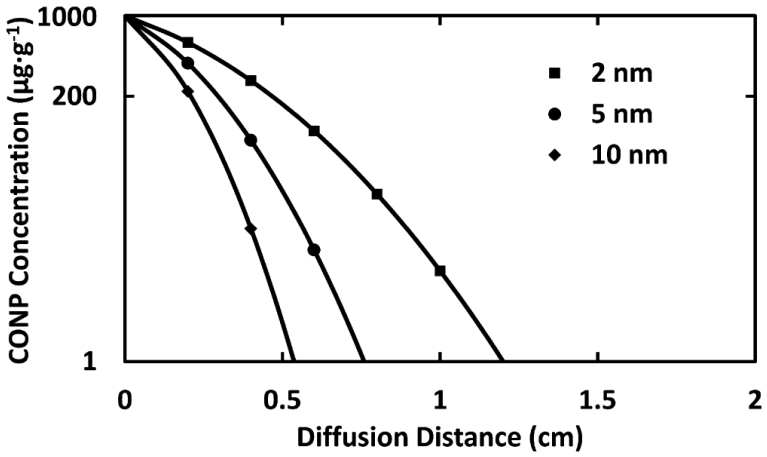

Figure 6.

CONP concentrations at distances ranging 0–2 cm from the initial source. Three sizes of nanoparticles were considered: 2, 5, and 10 nm. 5 ng-g^{-1} of CONPs were needed to eliminate ROS in the presence of 3.4 Gy. The values were obtained after seven days of diffusion.

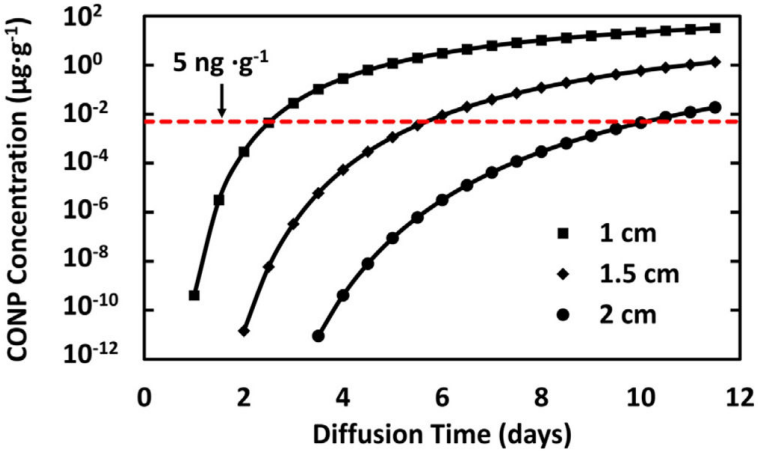

Figure 7.

Number of days need to achieve a CONP concentration (≥0.005 mg-g^{-1}) adequate to protect the tissue at a depth of 1, 1.5, and 2 cm.

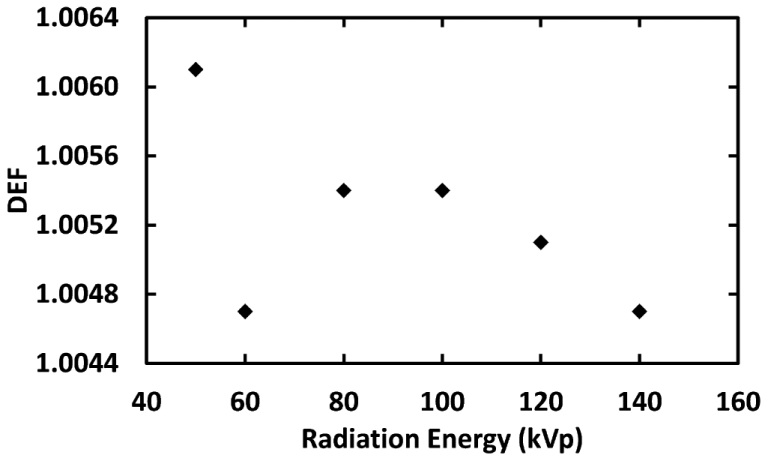

Figure 8.
DEF due to 0.645 mg-g^{-1} CONP with respect kVp radiation is less than 1.01.

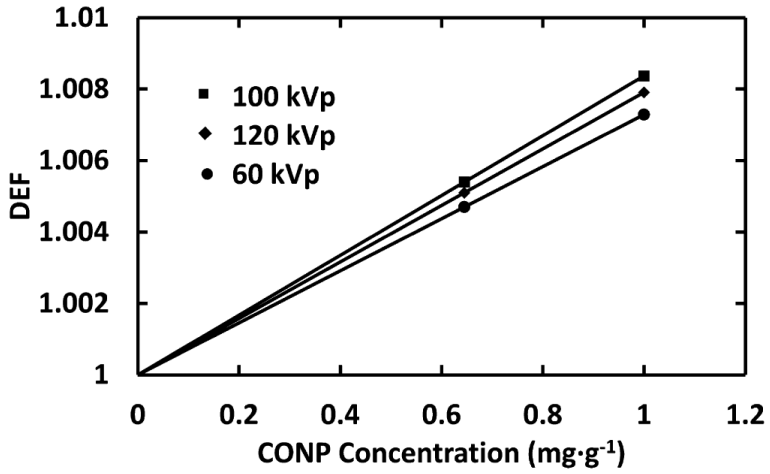

Figure 9.
DEF is linear with respect to CONP concentration at 60, 100, and 120 kVp.